JOURNAL OF MATERIALS SCIENCE 12 (1977) 1215–1224

Fatigue behaviour of ATJ graphite

R. E. BULLOCK
General Atomic Company, San Diego, California, USA

Detailed S–N curves are presented for two modes of fatigue testing characterized by different minimum-to-maximum stress ratios, R. The endurance limit, or maximum applied stress below which there were no failures, increased from 46% UTS for $R = -1$ to 64% UTS for $R = 0$, or from 116 to 162 kg cm^{-2}. Thus, as the stress range narrowed for a given maximum stress, the endurance limit increased with mean stress. For ATJ specimens of a given tensile strength σ_i, the smallest value of maximum applied stress, σ_A, at which fatigue cracks propagated was defined by σ_A/σ_i ratios of 0.60 and 0.85 for $R = -1$ and $R = 0$, respectively. In addition, selected fatigue tests were conducted for several mean compressive stresses in order to complete the definition of a Goodman diagram for ATJ graphite.

1. Introduction

The purpose of the work reported here was two-fold: (1) to determine if valid fatigue data could be generated from push–pull tests on a simple graphite specimen with parallel sides and, if so, (2) to obtain preliminary engineering-design data on fatigue of one of the several graphite candidates for use in the high-temperature gas-cooled reactor (HTGR). The core of an HTGR consists largely of graphite [1] comprising: (1) blocks for containing the nuclear fuel, (2) surrounding permanent side reflectors, (3) elevated floor slabs on which the blocks are stacked, and (4) underlying floor-support posts that provide the plenum area for circulation of helium coolant through the core. There are at least two candidate materials for each of these four major graphite components, and several of these materials need to be fatigue tested for at least three different environmental conditions: (1) elevated temperature, (2) irradiation exposure, and (3) pressurized helium atmosphere with low impurity levels of oxidants. Thus, there are several series of fatigue tests yet to be conducted on candidate graphites for the HTGR, and the use of a uniform specimen cored directly from graphite blocks would simplify this work considerably. However, uniaxial tensile testing of brittle materials is difficult [2–10], even under the best test conditions in which carefully designed specimens are used [9, 10], and a uniform specimen having inevitable stress concentrations [2–4] in push–pull testing must be shown to give valid fatigue data when properly normalized [4] if it is to be useful.

2. Experimental details

The graphite selected for study was Union Carbide's well-characterized ATJ graphite, which is a candidate material for core-support posts in the HTGR. This is a unidirectionally moulded graphite that is produced without re-impregnation; it has an average density of 1.74 g cm^{-3}, a maximum grain size of about 150 μm, and a between-grain pore size in the 3 to 4 μm range [11]. The nominal with-grain (WG) tensile strength of ATJ is 280 kg cm^{-2} and the across-grain (AG) strength is 240 kg cm^{-2},* each with about a 10% coefficient of variation (CV), while the minimum compressive strength is about 600 kg cm^{-2} [12]. Cylindrical samples with diameters of 0.648 and 1.28 cm were cored from the weaker central portion [11] of a well-characterized [13] 23 cm x 50 cm x 60 cm block of graphite that had been moulded along the thinner 23 cm direction, producing isotropic grain orientations in planes perpendicular to the pressing direction. These samples with lengths of 7.6 cm

* 1 kg cm^{-2} = 14.22 psi = 0.0981 MPa.

© 1977 Chapman and Hall Ltd. Printed in Great Britain.

were taken in the WG direction parallel to the 60 cm length, which corresponds to the axial direction of core-support posts. The smaller as-cored samples were later reduced to a diameter of 0.635 cm by centreless grinding, and then were cut into five 1.5 cm sections for fatigue testing. These uniform sections of graphite were subsequently aligned in elevated central notches within carefully machined V-blocks, and their overhanging ends were glued with epoxy resin into slightly larger 0.15 cm deep recesses within 1.27 cm cylindrical metal end fittings that were threaded internally on opposite ends for attachment into the fatigue machine. The freshly glued end fittings were rotated in their alignment channels to produce a smooth, uniform ring of epoxy around the graphite specimen; this is the specimen shown at the top of Fig. 1, with the small size of the uniform graphite insert being set in anticipation of future fatigue testing of companion specimens that will be irradiated in space-limited capsule experiments. Comparative testing was also done for the dumb-bell-type specimen shown at the bottom of Fig. 1; this was made by gradually machining down the larger cored samples to the same 0.635 cm diameter as for the uniform specimen.

These specimens were push–pull cycled in room-temperature air with the use of a direct-stressing fatigue machine (VSP-150) manufactured by Fatigue Dynamics Inc. The load applied to a specimen was set by adjusting the eccentricity of a variable-throw crank while monitoring the output from a tension–compression load cell that had been added to the machine, along with a carefully aligned test cage designed for tension–compression loading. Specimens were loaded smoothly by hand-turning the crank through the first 20 cycles to verify uniformity of load, and the speed of the drive motor was then brought up to 3 Hz for the 10^5 cycle duration of the test. This gave strain-rates of about 10^{-2} sec^{-1}, where several types of graphite have their lowest tensile strength [14]. The load was periodically monitored throughout each test, and it rarely varied by more than 3%.

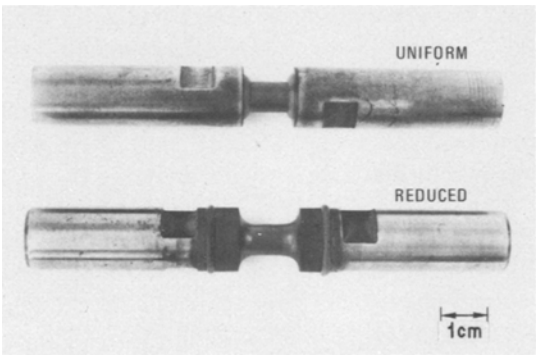

Figure 1 Two types of graphite fatigue specimens.

3. Results and discussion

The uniform specimen of Fig. 1 was the first type to be tested; 20 of these specimens were loaded continuously to failure in the fatigue machine to determine a tensile-strength distribution before any fatigue tests were run. This same type of specimen had been used in previous tensile tests of an extruded near-isotropic graphite candidate for HTGR fuel blocks [15], and roughly 75% of those failures occurred well within the gauge-length section of the graphite. However, it soon became apparent that ATJ failures almost invariably occurred through the graphite right at the outer epoxy boundary, and several refinements in loading alignment (such as allowing tacky epoxy bonds to cure in the fatigue machine after being lightly loaded) did nothing to change this. Apparently, unavoidable stress concentrations [4] were sufficient to dominate the normal weakest-link failure [16–20] of fine-grained ATJ graphite, but not of the much larger-grained (1500 μm maximum) near-isotropic graphite that had more-severe flaw sites.

To estimate the apparent strength reduction caused by the stress concentration at the abrupt attachment boundary of the uniform specimen, ten of the reduced-section specimens of Fig. 1 were tensile tested in the fatigue machine. The mean ultimate tensile strength (UTS) of these specimens increased by 20% to a value of 253 kg cm^{-2}, which agrees well with strength determinations of other investigators [21, 22]. The sets of n ordered strength values from tests on the two types of specimens are distributed along boundaries of $n + 1$ equal probability intervals on the left-hand side of Fig. 2 [16], and cumulative Weibull strength distributions [16, 17] obtained from these data by maximum likelihood estimates [23, 24] are observed to have almost identical shapes. Therefore, the strength distribution for reduced-section specimens is very little distorted by including uniform-specimen results that have been multiplied by the normalizing factor of 1.20, which brings mean strengths for the two specimen types into agreement as shown by the combined strength distribution (solid curve) on the right-hand side of

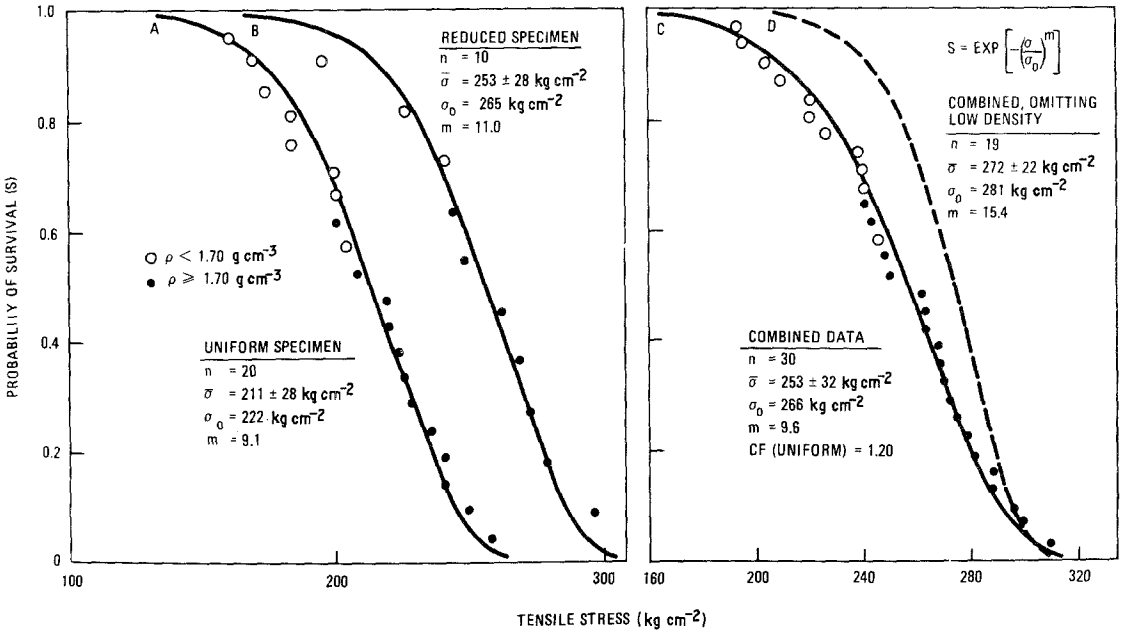

Figure 2 Weibull strength distributions for uniform and for reduced ATJ specimens.

Fig. 2. Hence, it was concluded that uniform specimens of the type more suited for space-limited capsule irradiations can be used to generate valid tensile data when stresses are multiplied by the experimental stress-concentration factor.

A very strong density effect on tensile strength is also apparent from an examination of the various sets of data points in Fig. 2. Solid and open circles denote specimens with densities above and below $1.70\,g\,cm^{-3}$, respectively, and low-density specimens are invariably clustered toward low-strength tails of the distributions. The dashed curve on the right-hand side of Fig. 2 is obtained by omitting the open-circled data for the lower density specimens. With the elimination of these weaker specimens, the UTS increases to $272\,kg\,cm^{-2}$ and the CV drops from 13 to 8%; this upward shift in value and reduction in scatter of the strength distribution should continue as higher and higher density specimens are omitted. Some idea as to strengths obtainable with increasing density beyond the range of current ATJ values can be gained by examining reported properties of ATJ-S graphite, which is an improved ATJ-type material that has been specially processed to produce a mean density of $1.83\,g\,cm^{-3}$ [25], as opposed to an ATJ density of $1.74\,g\,cm^{-3}$ [12]. The nominal WG UTS of this improved graphite is $360\,kg\,cm^{-2}$ and the CV is 7% [25], the latter being in good agreement with the 8% value for the censored ATJ specimens with densities of at least $1.70\,g\,cm^{-3}$ (curve D of Fig. 2). The 30% higher strength for ATJ-S is roughly the value that is predicted for a density of $1.83\,g\,cm^{-3}$ from a projection of the near-linear strength–density relationship for the 30 ATJ tensile specimens whose strengths are shown in curve C of Fig. 2. These strengths vary from $193\,kg\,cm^{-2}$ for the lowest density specimen tested ($1.66\,g\,cm^{-3}$) to $310\,kg\,cm^{-2}$ for the highest density one ($1.78\,g\,cm^{-3}$). From this comparison, the UTS for ATJ graphite would continue to shift upward toward ATJ-S values if its mean density could be increased, and the scatter in UTS would drop as the density variation about that mean narrowed.

Fatigue testing of uniform specimens was initiated at this point, after it had been determined that the stress concentrations present shift the strength distribution downward without serious distortion. The first mode of fatigue testing to be tried involved equal tension and compression cycles about a zero mean stress, i.e. the ratio of the minimum to the maximum applied stress was $R = -1$. The fatigue life for such testing is plotted in Fig. 3 as a function of the apparent maximum applied stress divided by the uncorrected mean strength of the uniform specimen ($211\,kg\,cm^{-2}$). The data of Fig. 3 represent fatigue tests of 71 specimens: 47 that failed and 24 that ran out to 10^5 cycles before testing was terminated. In

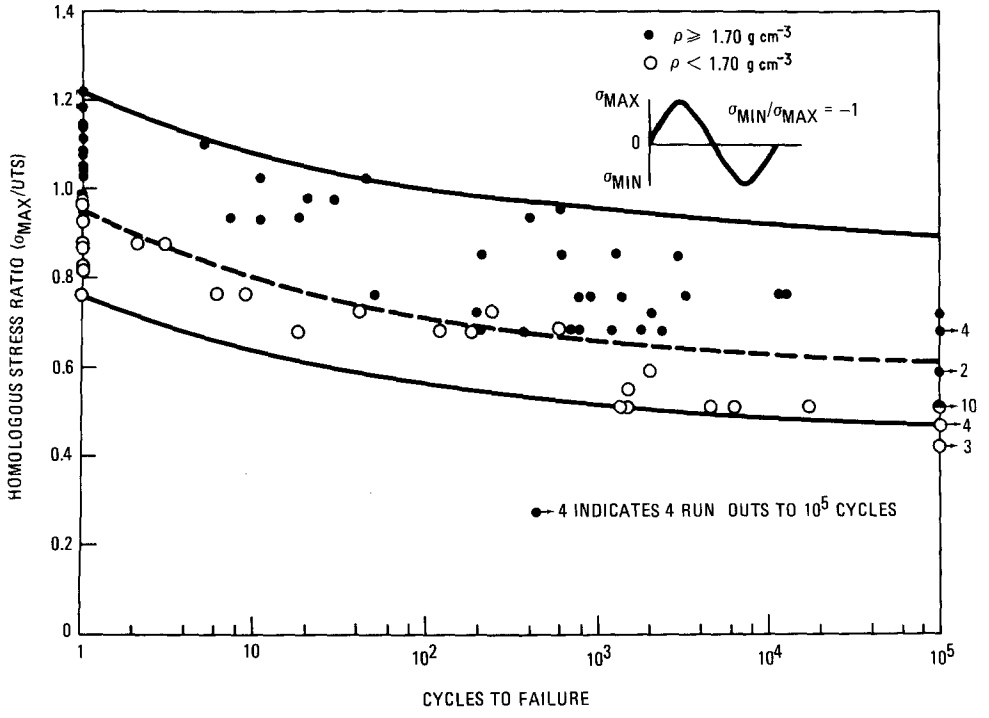

Figure 3 Normalized fatigue data for equal-cycle push–pull testing of uniform ATJ specimens.

addition, strengths of the 20 preselected tensile specimens are plotted along $N = 1$ to define the strength spread, and it is observed that when projected back to a single cycle the extremes of the fatigue band (solid curves) merge nicely with extreme values of the tensile strength. Moreover, the width of the fatigue band along the stress axis is essentially uniform for all values of N, which indicates that it is the scatter in tensile strength that largely determines the width of the fatigue band throughout its range. Thus, there appears to be a unique S–N fatigue curve [26–28] for all specimens having a common tensile strength, and it is the scatter in tensile strength that smears this curve out over the width of the fatigue band. Therefore, if the strength distribution could be narrowed, as for ATJ-S graphite, the fatigue band should narrow down in proportion. This interpretation is supported by an examination of specimens that have been segregated into densities above and below 1.70 g cm^{-3}. The higher density (solid) data points of Fig. 3 all fall in the upper two-thirds of the fatigue band above the dashed curve, and this narrowed band then merges with tensile strength extremes of higher density (solid) points along $N = 1$; the same situation holds for the lower density (open circle) data in the lower one-third of the fatigue band.

Finally, it is observed from Fig. 3 that no fatigue failures occur within 10^5 cycles for specimens that are cycled at maximum stresses below 46% UTS; this is in excellent agreement with reported endurance limits of 47% [29] and 49% [30] UTS for reverse bending of high density graphites. Likewise, by monitoring fatigue crack propagation in compact tension specimens, an endurance limit of about 50% UTS has been deduced for both a pressed high density graphite and an extruded lower density one [31]. Therefore, many graphites have essentially the same endurance limit for a given mode of fatigue testing when applied stresses are expressed as percentages of the mean tensile strengths for the graphites in question, as observed by Leichter and Robinson [29]. However, it appears from the data given here that the endurance limit more properly rises and falls with the lowest value of the tensile strength rather than with the mean of the distribution. Censored specimens of Fig. 3 with densities greater than 1.70 g cm^{-3} have a mean strength (σ_u) of 1.08 UTS and an endurance limit of about 0.6 UTS, for example, so that the endurance limit increases from 46% UTS for the entire population to 56% σ_u for the censored population (solid points). However, in both cases, the endurance limit is about 60% of the strength of the weakest tensile specimen. The minimum

and the mean strength values change in the same proportion when a distribution shifts without change of shape, as occurs when the same graphite is fatigue tested at different temperatures [32, 33] or when different graphites with similar scatter in tensile strength are fatigue tested at the same temperature [29, 30], and the mean value of a distribution can be determined much more precisely than can its extreme values. Therefore, for practical purposes, it is probably best to normalize applied fatigue stresses by mean strength values unless shapes of the cumulative strength distributions of the graphites being compared are known to differ significantly, as in the right-hand side of Fig. 2.

In addition to the endurance limit being 60% of the strength of the weakest specimen tested,* it should also be noted that the highest run-out stress of Fig. 3 (0.72 UTS) is about 60% of the strength of the strongest specimen tested. Thus, it appears that an ATJ specimen cycled about a zero mean stress will almost always run out to 10^5 cycles provided that the maximum applied stress, σ_A, does not exceed 60% of the individual specimen strength, σ_i, and it will almost always fail if cycled above that value. This interpretation is supported by examining σ_A/σ_i ratios for the 24 run-out specimens of Fig. 3 that were loaded to failure without ever being removed from the fatigue machine. The highest ratio found was 0.61, which implies that all specimens with higher ratios had failed. When this ratio is applied to the weakest tensile specimen (0.76 UTS), the maximum applied stress at which a runout can be obtained is 0.46 UTS, but from Fig. 3 this is also the minimum applied stress at which a failure can be obtained. Therefore, there must be a sharp threshold stress for a given specimen (equivalent to about 60% of its individual strength) above which failure almost always occurs within 10^5 cycles and below which it rarely occurs.

Next, ten of the reduced-section specimens were cycled to verify that they define a fatigue band of the same shape as that for uniform specimens. These data are plotted in Fig. 4 without normalization (triangular points), and the dashed lines containing all such points define a fatigue band of near-constant width along the stress axis that merges well with extreme values of tensile strength (at $N = 1$) for similar reduced specimens. The data of Fig. 3 for uniform specimens are now

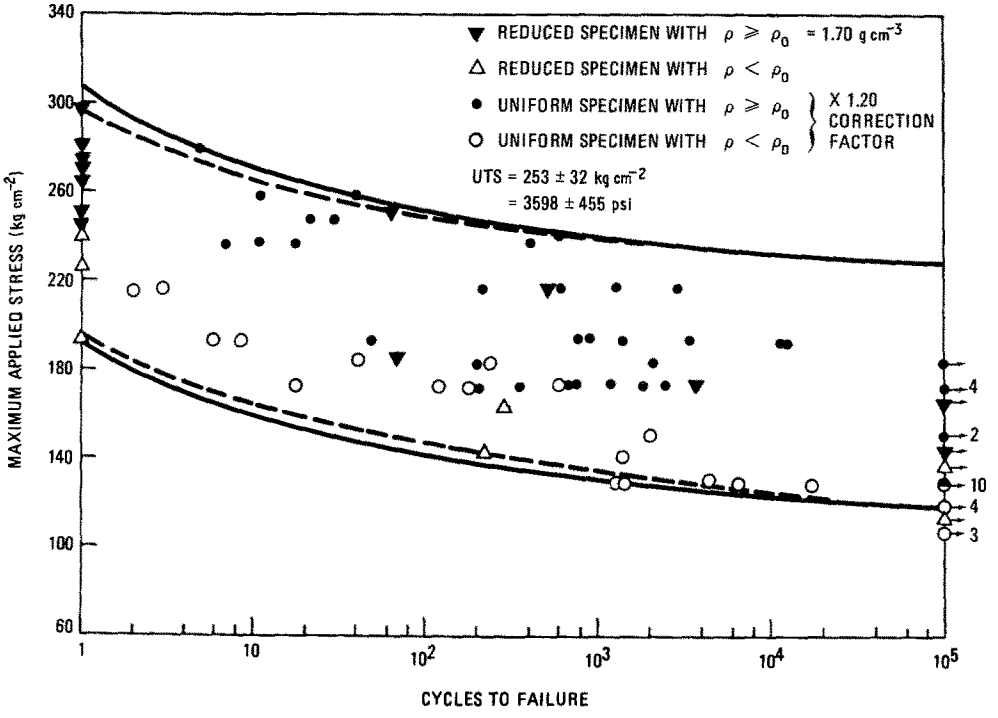

Figure 4 Fatigue of with-grain ATJ graphite for push–pull cycling with $R = -1$.

* The endurance limit given here is arbitrarily defined to be the stress value at the point where the lower boundary of the fatigue band intersects 10^5 cycles; this represents roughly a 1% failure probability within that range for the data of Fig. 3.

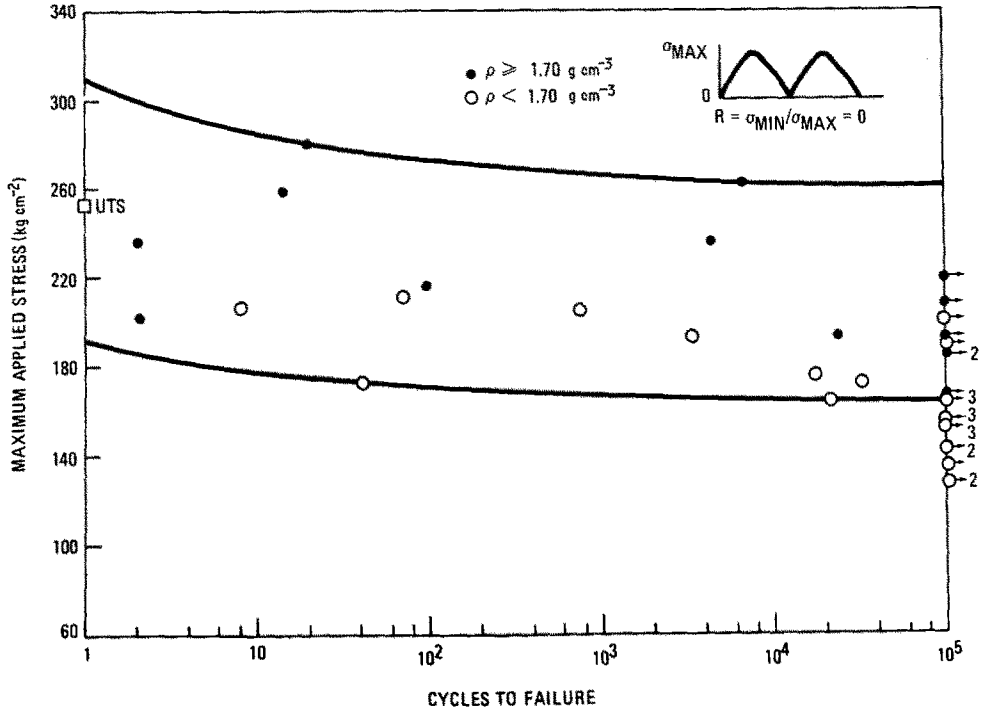

Figure 5 Fatigue of with-grain ATJ graphite for push–pull cycling with $R = 0$.

replotted (circled points) in terms of actual applied stress after having been multiplied by the stress-concentration factor of 1.20, and the solid lines define the slightly wider boundaries of their fatigue band. Both sets of data define essentially the same fatigue band, however, and the endurance limit of 0.46 UTS at 10^5 cycles now assumes the absolute value of 116 kg cm^{-2}. Even though data for reduced-section specimens are skimpy, the similarities in shapes of the fatigue bands are clear. Again, near-60% values are obtained for both the ratio of the highest run-out stress to the strongest tensile specimen and the ratio of the endurance limit to the weakest tensile specimen. Moreover, the highest σ_A/σ_i ratio from tests on the four runout specimens was 0.59, as compared to 0.61 for the uniform specimen. Thus, the fatigue band for uniform specimens has been brought into excellent agreement with that for reduced-section specimens by multiplying both the apparent tensile strength and the apparent fatigue stress by the experimental stress-concentration factor of 1.20 that was determined from tension tests. Similar fully notch-sensitive behaviour in fatigue has been reported for several types of brittle composite materials [34].

Uniform specimens, whose use in fatigue tests of ATJ graphite had now been justified, were tested next in a second mode of fatigue ($R = \sigma_{min}/\sigma_{max} = 0$) to judge the influence of mean stress on fatigue life; these data are shown in Fig. 5, where the same stress-concentration factor has been applied. The endurance limit increased to 162 kg cm^{-2}, or 64% UTS, for these tests in which the compressive phase of the cycle was omitted. This agrees well with the 68% limit obtained from similar testing of a near-isotropic core graphite [15] and with the approximate 70% value implied from tensile fatigue of a finer grained graphite [4]. Thus, as the cyclic stress range narrows for a given applied peak stress, the endurance limit increases along with the mean stress. The highest σ_A/σ_i ratio found from among the 22 run outs for $R = 0$ was 82%, and this agrees well with the 85% value found for the ratio of the endurance limit to the weakest tensile specimen. However, the ratio of the highest run-out stress to the strongest tensile specimen was only 71%, which indicates that a higher run-out stress could probably be obtained with additional testing. An 85% value is exactly what is needed to elevate the highest run-out stress to the very top of the fatigue band. Thus, it appears that an ATJ specimen will almost always run out to 10^5 cycles for testing with $R = 0$ provided that the maximum applied stress does not exceed 85% of the individual specimen strength, and it will

almost always fail if cycled at higher stresses. The corresponding critical stress ratio for crack propagation with $R = -1$ was only 60%.

The data of Figs. 4 and 5 were analysed by Weibull techniques [29] to produce the 50% failure curves of Fig. 6 for the two test conditions in question. The median fatigue life for the positive mean-stress condition ($R = 0$) is greater than that for zero mean stress ($R = -1$) for all maximum applied stresses below the median tensile strength ($\approx$ UTS), and this difference in fatigue life becomes greater as stresses are lowered toward endurance limits. The data points of Fig. 6 were obtained in a two-step process. First, the fatigue envelopes of Figs. 4 and 5 were arbitrarily divided into 7 and 3 stress bands, respectively, each band being associated with a single peak stress (σ_p) equal to its mid-range value. Then, without regard to first-cycle failures, values of N for the k failures from among the n fatigued specimens falling within each of these bands were used in an iterative computer procedure to obtain maximum likelihood estimates for the parameters m and N_o in the cumulative Weibull fatigue distribution [35, 36]

$$S_f = \exp(-N/N_o)^m,$$

where S_f is the probability that a specimen will survive N cycles to a peak stress of σ_p. Here, the $r = n - k$ run-out specimens in the band were distributed at values of $S_f = i/(n+1)(i = 1, \ldots, r)$ along the long-life tail of the resulting $S_f(N)$ distribution, or, in effect, were analytically failed at some number of cycles beyond the actual 10^5 cut-off point. Second, the probability S_1 for first-cycle survival at the σ_p stress appropriate for each band was obtained from curve C of Fig. 2, and the number of fatigue cycles required to reduce the $S_1 S_f$ product to $\frac{1}{2}$ was calculated from

$$N = N_o[\ln 2S_1]^{1/m};$$

these are the values of N for median fatigue life that are plotted in Fig. 6 for each stress band into which the data of Figs. 4 and 5 had been divided. The number of data points in Fig. 4 at a single stress value was adequate for analysis in several cases, without the need for setting a band width and working with an average stress value [37]; these values are shown by solid data points. The arbitrary projections beyond the last calculated points (dashed segments) indicate only that median failure curves should level out to values that are greater than the endurance limits indicated.

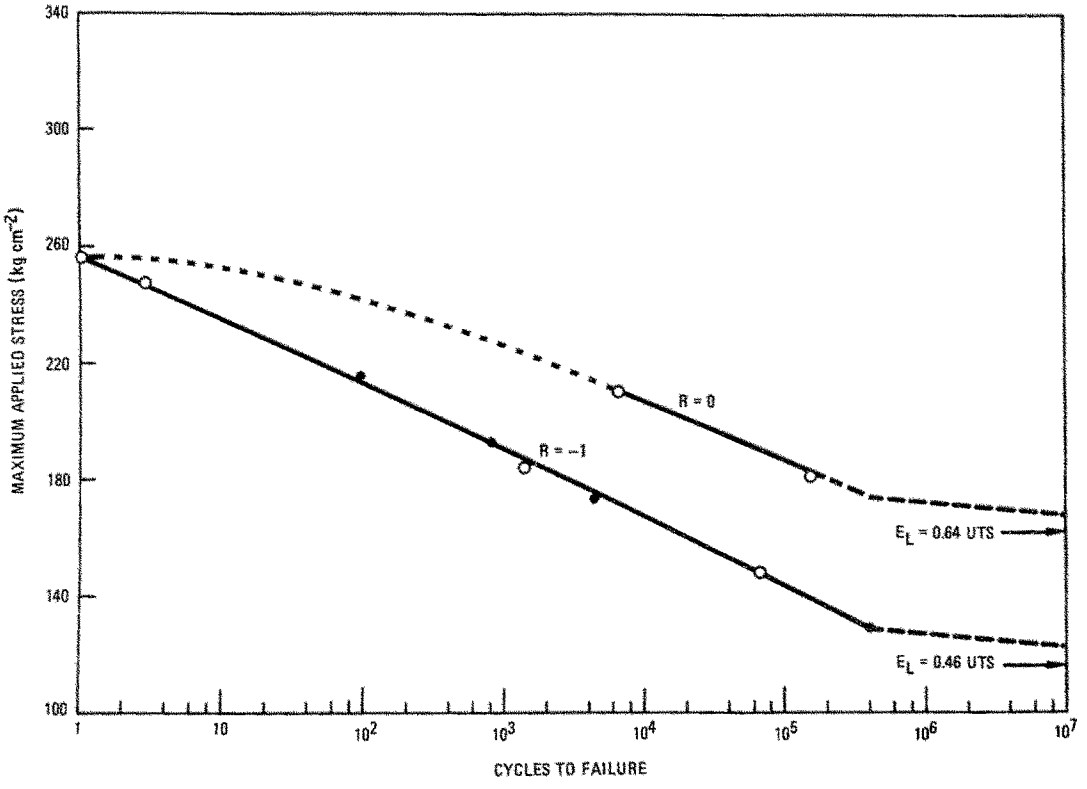

Figure 6 Stress–lifetime plots for 50% failure probabilities of ATJ graphite under two test conditions.

The median lifetime data of Fig. 6 are replotted in terms of a mean stress with a superimposed symmetrical stress amplitude in the right-hand half of the Goodman diagram of Fig. 7. Some fatigue testing was also done for mean compressive stresses, and these data are shown plotted along the dashed projection in the left-hand half of the diagram. In particular, seven points along the projection of the 50% failure curve for 10^5 cycles were checked out very roughly by running three or four specimens for those conditions, half of which should be expected to fail, and the ratios of r/n given indicate the number of run outs r that were obtained in the n tests at the point in question. In total, 13 of the 24 specimens tested ran out to 10^5 cycles, which indicates that the projected curve cannot be too much in error. In a side experiment on static fatigue, ten specimens were loaded to UTS and held there for 65 h (a time sufficient for the completion of 7×10^5 cycles at a rate of 3 Hz), and none of these failed. While this test was not very meaningful statistically, it does indicate that static fatigue effects are small for ATJ graphite, in agreement with findings for another graphite [38]. Therefore, based on the limited data available, the 50% failure curves of Fig. 7 are all shown to cut the $R = 1$ axis at UTS, but additional static testing might well cause a slight reduction of this intercept value for the higher cycle curves.

4. Conclusions

(1) Valid tensile and fatigue data can be obtained from testing of uniform ATJ specimens, provided that results are properly normalized by experimental stress-concentration factors.

(2) There is a strong density effect on the tensile strength and fatigue life of this graphite, both of which increase sharply with density.

(3) Scatter in tensile strength largely determines the width of the S–N fatigue band along the stress axis S, and the endurance limit is determined by the specimen having the lowest tensile strength.

(4) The endurance limit increases from 46% UTS for a stress ratio of $R = -1$ to 64% UTS for $R = 0$, or from 116 to 162 kg cm^{-2}.

(5) For endurance limits to remain invariant, however, applied fatigue stresses should be normal-

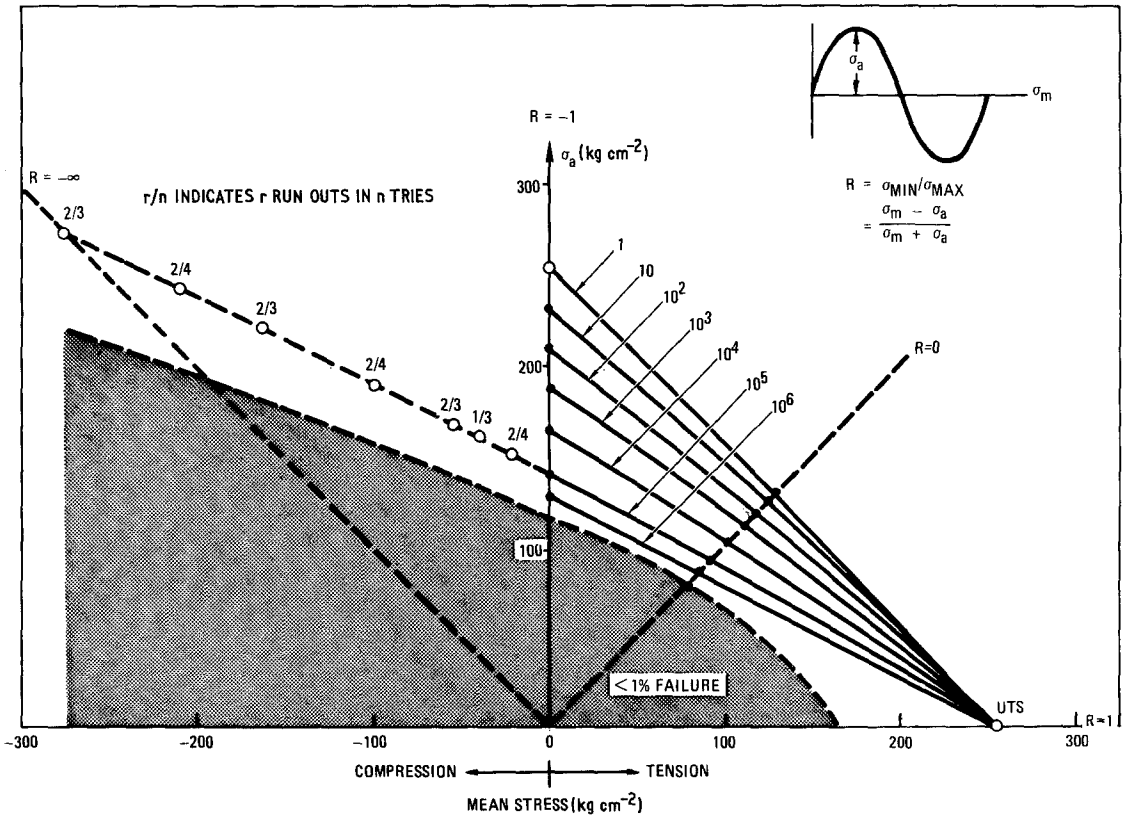

Figure 7 Goodman diagram showing 50% failure curves for ATJ graphite.

ized in terms of the weakest tensile specimen (WTS), rather than the mean strength of the distribution (UTS). When this is done, the endurance limit becomes 60% WTS for $R = -1$ and 85% WTS for $R = 0$.

(6) In fact, for ATJ specimens of any given tensile strength σ_i, run outs to 10^5 cycles will almost always be obtained for $R = -1$ provided that the maximum applied stress σ_A does not exceed 60% σ_i, while failure within that range is almost certain for any higher stress. Likewise, $\sigma_A/\sigma_i \approx 0.85$ defines the crack-propagation threshold for $R = 0$. An examination of σ_A/σ_i values for the two types of runout specimens supports these conclusions.

(7) The median fatigue life of graphite depends on both the maximum and the mean stress during a cycle. As the stress range narrows for a given maximum stress, the fatigue life increases with the mean stress.

(8) The amplitude of cyclic stress required to produce 50% failure within a given number of cycles increases sharply as the mean stress about which it is imposed moves toward compressive values.

(9) The mean strength of specimens that survived 10^5 cycles was 6% higher than that of the original population. There was no upward shift of the high-strength portion of the original distribution [39], however, only a truncation of lower-strength specimens through fatigue proof testing [40].

Acknowledgements

The author gratefully acknowledges the skillful experimental assistance provided by Mr T. Tagami during all phases of this work. Appreciation is also expressed to Drs R. J. Price and G. H. Reynolds for valuable suggestions on experimental design, to Mr J. B. Wattier for programming the MLE procedure for calculating Weibull parameters, and to Messrs D. I. Roberts and J. E. Sheehan for useful suggestions on data presentation.

References

1. D. A. NEHRIG, A. J. NEYLAN and E. O. WINKLER, Conference on Graphite Structures for Nuclear Reactors, London (March 1972) p. 185.
2. W. H. DUCKWORTH, *J. Amer. Ceram. Soc.* **34** (1951) 1.
3. A. RUDNICK and W. H. DUCKWORTH, Conference on Nuclear Applications of Nonfissionable Ceramics, Washington, D.C. (May 1966) p. 453.
4. D. K. BAZAJ and E. E. COX, *Carbon* **7** (1969) 689.
5. I. B. MASON, "Proceedings of the Fifth Conference on Carbon", Vol. 2 (Pergamon Press, New York, 1960) p. 597.
6. N. A. WEIL and I. M. DANIEL, *J. Amer. Ceram. Soc.* **47** (1964) 268.
7. D. R. PLATTS and H. P. KIRCHNER, *J. Materials* **6** (1971) 48.
8. R. BERENBAUM and I. BRODIE, *Brit. J. Appl. Phys.* **10** (1959) 281.
9. R. L. BARNETT and R. L. McGUIRE, *Amer. Ceram. Soc. Bull.* **45** (1966) 595.
10. H. E. SHULL, *ibid* **55** (1976) 202.
11. "The Industrial Graphite Engineering Handbook", Carbon Products Division of Union Carbide Corporation (1964).
12. Union Carbide Technical Information Bulletin No. 463-205ej on Premium Graphite Grade ATJ.
13. K. KOYAMA, General Atomic Company, private communication (April, 1976).
14. J. S. EVANGELIDES, 12th Biennial Conference on Carbon, Pittsburgh (July 1975) p. 91.
15. R. E. BULLOCK, 12th Biennial Conference on Carbon, Pittsburgh (July, 1975) p. 141.
16. W. WEIBULL, *Ing. Vetenskaps Akad. Handl.* **151** (1939).
17. W. WEIBULL, *J. Appl. Mech.* **18** (1951) 293.
18. B. EPSTEIN, *J. Appl. Phys.* **19** (1948) 140.
19. D. E. GÜCER and J. GURLAND, *J. Mech. Phys. Solids* **10** (1962) 365.
20. "Ceramic Processing", National Academy of Science Publication 1576 (1968) p. 245.
21. C. A. ANDERSSON and E. I. SALKOVITZ, in "Fracture Mechanics of Ceramics", Vol. 2, edited by R. C. Bradt, D. P. H. Hasselman and F. F. Lange (Plenum Press, New York, 1974) p. 509.
22. G. T. YAHR and R. S. VALACHOVIC, *ibid*, p. 863.
23. J. W. HEAVENS and P. N. MURGATROYD, *J. Amer. Ceram. Soc.* **53** (1970) 503.
24. D. G. S. DAVIES, *Proc. Brit. Ceram. Soc.* **22** (1973) 429.
25. Union Carbide Technical Information Bulletin No. 463-201hi on Graphite Grade ATJS.
26. B. J. S. WILKINS, *J. Materials* **7** (1972) 251.
27. B. J. S. WILKINS and A. R. REICH, *Amer. Ceram. Soc. Bull.* **51** (1972) 486.
28. B. J. S. WILKINS, in "Fracture Mechanics of Ceramics", Vol. 2, edited by R. C. Bradt, D. P. H. Hasselman and F. F. Lange (Plenum Press, New York, 1974) p. 875.
29. H. L. LEICHTER and E. ROBINSON, *J. Amer. Ceram. Soc.* **53** (1970) 197.
30. V. N. BARABANOV, Y. P. ANUFRIEV, G. G. ZAITSEV and M. Y. PIMKIN, *Ind. Lab. (USSR)* **32** (1966) 567.
31. P. MARSHALL and E. K. PRIDDLE, *Carbon* **11** (1973) 541.
32. L. GREEN, *J. Appl. Mech.* **18** (1951) 345.
33. M. GATEAU, G. SERTOUR, M. R. EVERETT and L. J. HANKART, Dragon Project Report DP-888 (June 1974).

34. R. B. HEYWOOD, "Designing Against Fatigue of Metals" (Reinhold, New York, 1962) p. 77.
35. ASTM Special Technical Publication No. 91-A (ASTM, Philadelphia, 1963) Appendix IV.
36. P. H. WIRSCHING and J. T. P. YAO, *J. Struct. Div. ASCE* **96** (1970) 1201.
37. R. PLUNKETT, in ASTM Special Technical Publication No. 121 (ASTM, Philadelphia, 1951) p. 45.
38. B. J. S. WILKINS, *J. Amer. Ceram. Soc.* **54** (1971) 593.
39. R. B. MATTHEWS, *ibid* **57** (1974) 225.
40. J. W. DALLY and L. N. HJELM, *ibid* **48** (1965) 338.

Received 6 July and accepted 5 October 1976.